frontiers | Frontiers in Earth Science

TYPE Original Research
PUBLISHED 25 July 2022
DOI 10.3389/feart.2022.963316

OPEN ACCESS

EDITED BY
Hu Li,
Southwest Petroleum University, China

REVIEWED BY
Cunhui Fan,
Southwest Petroleum University, China
Shun He,
Southwest Petroleum University, China

*CORRESPONDENCE
Bo Zhang,
zhangbo1934@163.com

SPECIALTY SECTION
This article was submitted to Structural Geology and Tectonics, a section of the journal Frontiers in Earth Science

RECEIVED 07 June 2022
ACCEPTED 06 July 2022
PUBLISHED 25 July 2022

CITATION
Luan B, Zhang B, Wang D, Deng C and Wang F (2022), Quantitative evaluation of tight oil reservoirs in the Chang 8 Member of the Yanchang Formation in southern Ordos Basin.
Front. Earth Sci. 10:963316.
doi: 10.3389/feart.2022.963316

Quantitative evaluation of tight oil reservoirs in the Chang 8 Member of the Yanchang Formation in southern Ordos Basin

Beibei Luan[1], Bo Zhang[2]*, Didong Wang[1], Chao Deng[3] and Feng Wang[4]

[1]Development Department, Yanchang Oifield Co., Ltd., Yan'an, Shaanxi, China, [2]Zhidan Oil Production Plant, Yanchang Oilfield Co., Ltd., Zhidan, Shaanxi, China, [3]Yulin Refinery, Yanchang Petroleum (Group) Co., Ltd., Jingbian, Shaanxi, China, [4]Jingbian Oil Production Plant, Yanchang Oilfield Co., Ltd., Jingbian, Shaanxi, China

The precise and quantitative characterization of reservoir properties is the key to efficient development of tight oil reservoirs. In this paper, taking the Chang 8 Member of the Yanchang Formation in the Shuimogou area in the southern Ordos Basin as an example, the sedimentary facies types, microscopic pore structures, diagenesis, influencing factors of physical properties, and hydrocarbon enrichment law of tight oil reservoirs are systematically studied. The research results show that the Chang 8 Member in the study area is a typical delta front subfacies deposit, including distributary channel and inter-distributary bay microfacies. The constructive diagenesis of the Chang 8 Member include dissolution, metasomatism and rupture; while the destructive diagenesis include mechanical compaction and cementation. The Chang 8 reservoir has entered the middle diagenetic stage A. The factors affecting the physical properties of tight oil reservoirs include deposition, compaction, cementation and dissolution. The secondary pores formed by dissolution account for 10–40% of the total surface porosity, with an average value of 24%. Local structures and sediments have significant control over hydrocarbon accumulation. The westward dipping tectonic setting of the northern Shaanxi Slope provides the basic conditions for the migration of oil and gas to the eastern updip areas. The changes of lithology and physical properties in the updip direction of the structure form the blocking conditions for the continued migration of oil and gas, which is conducive to the accumulation of oil and gas. In addition, the main oil reservoirs are mainly distributed along the distributary channel of the delta front, and most of the distributary channel sandstone is more than 20 m thick. The areas of thick sand body with multiple layers in the lateral direction is the main part of oil and gas accumulation. However, the reservoirs formed on the flanks of underwater distributary channels are generally thin and poorly sorted, which is not conducive to the accumulation of hydrocarbons.

KEYWORDS

reservoir evaluation, tight oil reservoirs, pore type, diagenesis, physical properties

Introduction

After more than a decade of exploration and research on tight oil exploration in China, rich areas of tight oil have been found in the Qingshankou Formation of the Songliao Basin, the Yanchang Formation of the Ordos Basin, and the Jurassic of the Sichuan Basin. Since 2010, based on the theory of "continuous hydrocarbon accumulation", the exploration thinking of tight oil in China has changed from "oil traps" to "entering oil sources". Later, the Changqing Oilfield has built China's first industrially produced tight oil area in the Ordos Basin. In 2013, a demonstration base for efficient development of tight oil in Xinjiang Oilfield was built. In 2015, the Xinanbian Oilfield, the first large-scale tight oil field of 100 million tons, was discovered in the Ordos Basin. In 2019, the one billion ton Gyeongseong Oil Field was discovered. At present, the Ordos Basin has the largest demonstration base for tight oil development in China (Yan, 2020).

With the decrease of conventional oil and gas resources, the exploration and development of tight oil and gas resources has attracted more and more attention (Cai, 2020; Curtis et al., 2012; Hong et al., 2020). There are abundant tight sandstone oil resources in the Upper Triassic Yanchang Formation in the Ordos Basin in the central China. The large-scale accumulation of oil and gas resources in the Yanchang Formation did not undergo long-distance migration. In recent years, with the developments of horizontal wells and fracturing technology, tight oil reservoirs of the Yanchang Formation has achieved great process (Houben et al., 2013; Li., 2022; Liu et al., 2021a). Evaluation of resource potential of tight oil depends on the accurate evaluation of various reservoir parameters (Li et al., 2019; Nie et al., 2020; Lan et al., 2021). Fine and quantitative characterization of reservoirs combining various advanced experimental and interpretation techniques is the key to efficient development of tight oil reservoirs (Anovitz et al., 2013; Cao et al., 2020; Chalmers et al., 2009).

In this paper, taking the Chang 8 Member of the Yanchang Formation in the Shuimogou area in the southern Ordos Basin as an example, the sedimentary facies types, microscopic pore structures, diagenesis, influencing factors of physical properties, and hydrocarbon enrichment law of tight oil reservoirs are systematically studied using the data of core, thin section, scanning electron microscope, X-ray diffraction, physical properties, oil testing and well logging. This study can provide a scientific basis for the rational and effective development of tight oil reservoirs.

Geological background

The study area is located in the Shuimogou Block of the Fuxian exploration area in the Ordos Basin (Figure 1A). The entire Upper Triassic Yanchang Formation in the study area is a west-dipping monocline, on which a series of low-amplitude uplifts developed (Figure 1B). The marker layers of the Chang 8 Member include K0, K1 and the middle mudstone (Figure 1C):

(1) Lijiapan Shale K0

The top interface of the K0 mark layer is the boundary between the Chang 8 and Chang 9 Members, and its thickness is generally 4–8 m. The lithology include black mudstone and shale, and the electrical characteristics are characterized by high natural gamma, high spontaneous potential, blocky high value of acoustic time difference, and relatively high resistivity (Figure 1C).

(2) Zhangjiatan Shale K1

The Zhangjiatan Shale is a thick oil shale segment. Its electrical characteristics are characterized by high acoustic time difference, high natural gamma, and high resistivity. It is an extremely important source rock marker layer distributed in the Ordos Basin (Figure 1C).

(3) Middle mudstone marker layer

The main lithology is gray-black mudstone, and its electrical properties are characterized by high acoustic time difference, high natural gamma, and high resistivity, and are widely developed in this area (Figure 1C).

From the statistical results, the burial depth of the Chang 8 Member in the study area is mainly between 1,300 and 1700 m, with an average burial depth of 1,500 m. The thickness of the Chang 8_1 sub-member is mainly between 40 and 60 m, with an average thickness of 53.4 m; and the thickness of the Chang 8_2 sub-member is mainly between 30 and 50 m, with an average thickness of 45.7 m.

On the basis of the identification of marker layers, wells with different positions, appropriate locations, and complete logging data are selected as comparison standard wells, and stratigraphic division is carried out in combination with rock debris, cores, gas logging and logging data (Li et al., 2012; Chen et al., 2021). The stratigraphic division adheres to the principle of "sedimentary cycle comparison". In this study, the stratigraphic division and comparison of 267 wells in the whole area have been completed, and a stratigraphic division and comparison database has been formed.

Materials and methods

Experimental test items include thin section, scanning electron microscope, X-ray diffraction, physical properties tests. Thin sections and scanning electron microscopy were used to analyze mineral composition, pore structures, and

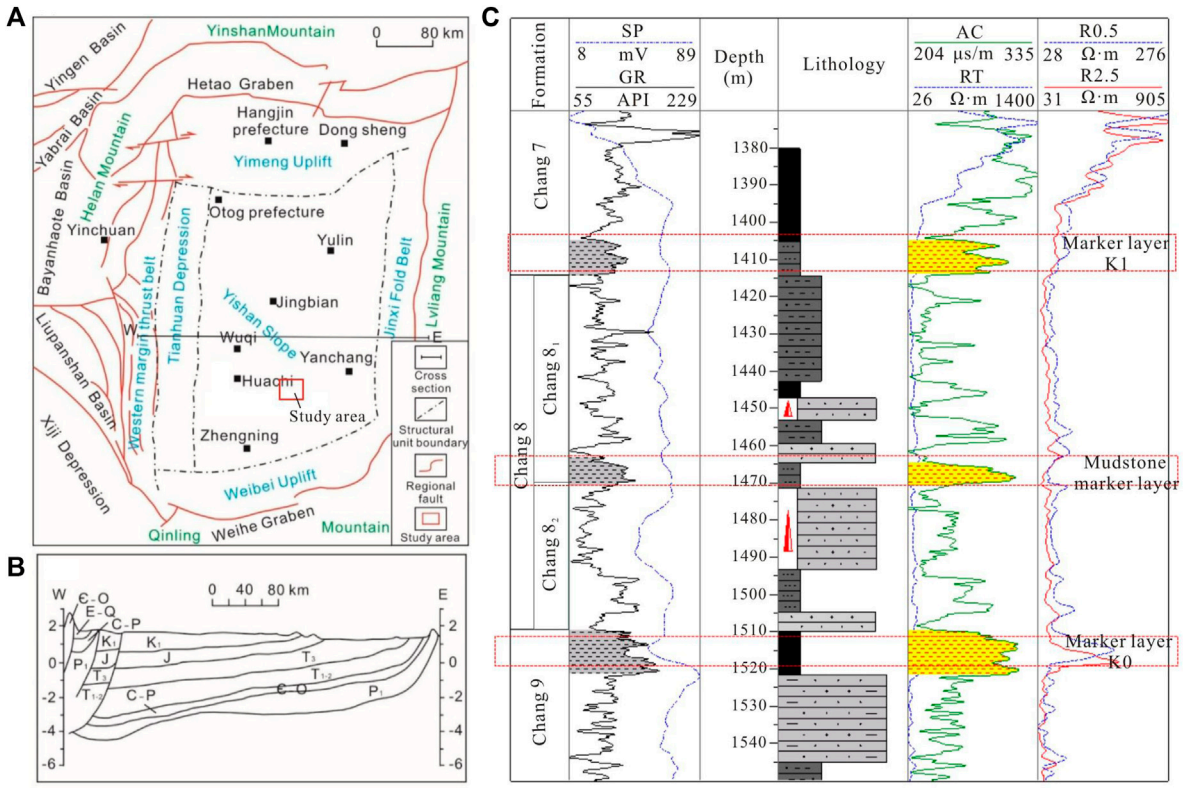

FIGURE 1
Location of the study area and division of the stratigraphic units of the Chang seven to Chang nine Members. **(A)** Location of the study area (Modified after Xiao et al., 2019); **(B)** East-west stratigraphic profile through the central part of the Ordos Basin; **(C)** Stratigraphic unit division of Chang seven to Chang nine Members.

surface porosity. X-ray diffraction experiments were used to determine the composition, crystal structure and content of various minerals and clays in the samples. The X-diffraction experimental instrument is a DMAX2500X diffractometer. Its 2θ angle measurement range: 10° ~ +154°; scanning step: 0.002°–90° (2θ/θ scan); 0.001°–90° (2θ scan); scanning speed: 0.002–100°/min (2θ/θ scan); 0.001°–100°/min (2θ scan). The instrument for physical property testing is a physical property testing system.

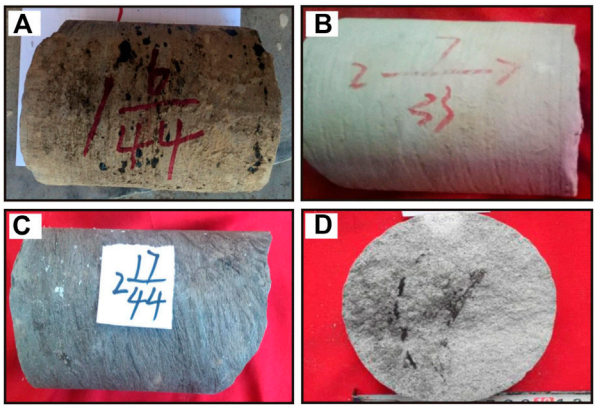

FIGURE 2
Sedimentary structures of the Chang 8 Member of Yanchang Formation in the study area. Notes: **(A)** Oil trace fine sandstone, Well L144, 1195.81 m; **(B)** Parallel bedding, Well L149, 1535.15 m; **(C)** Deformation bedding, Well L143, 1526.98 m; **(D)** Plant carbon fractions, Well L96, 1,526.98 m.

Results

Sedimentary facies type

The sedimentary facies markers should have special lithology in the vertical direction, and the electrical measurement curves should reflect clearly the special sedimentary environment (Bieniawski., 1967; Chalmers and Bustin., 2007; Chen et al., 2016). Therefore, it should have the characteristics of stable thickness and extensive development in the lateral direction.

That is to say, as a sedimentary facies marker of a sedimentary basin, it should not only be regionally extensive, but also have easy-to-identify characteristics (Lorenz and Finley., 1991; Lai and Wang., 2015; Lai et al., 2018; Mahmud et al., 2020).

(1) Color

Core observations show that the medium-fine sandstone and siltstone in the Yanchang Formation in the study area are gray-white and dark gray, and the mudstone is gray, gray-black, and black (Figure 2). It reflects that the target layer was a weak reduction-reduction depositional environment at that time (Liu et al., 2015; Mahmoodi et al., 2019; Liu B et al., 2020; Radwan., 2022).

(2) Special sedimentary structures

Parallel bedding, wavy bedding, sand-mud rhythmic bedding, and trough-like cross bedding can be seen widely in the cores of the target layer; however, contemporaneous deformation structures, carbonized plant debris, and thin coal seams can be seen in very few cores (Figure 2).

(3) Authigenic minerals

Although authigenic minerals are usually low in terrigenous clastic rocks. However, authigenic pyrite crystals are common in the mudstone of the Chang 8 Member in the study area, reflecting a strong reduction environment in deeper water.

The Chang 8 Member in the study area developed delta front subfacies, including underwater distributary channel and interdistributary bay microfacies. The delta front is located between the lake surface and the wave base, and is not only the main part of the delta deposition, but also the areas where the sandy sediments in the delta depositional facies are concentrated (Xiao et al., 2019; Liu J et al., 2020; Santosh and Feng., 2020; Radwan et al., 2021; Liu et al., 2022). According to different sedimentary characteristics and sedimentary facies markers, two microfacies of underwater distributary channel and inter-distributary bay were identified in Chang 8 Member of the study area. Among them, the underwater distributary channel has deposited large-scale sand bodies, which are the "main body" of the delta front.

The underwater distributary channel is the continuous extension of the distributary channel on the delta plain to the underwater, and the bottom of the channel is washed by water (Shuai et al., 2013; Shanley and Cluff 2015; Xu et al., 2021; Yin et al., 2018). Relatively coarse-grained fine-siltstone is found near the main channel, and relatively fine-grained siltstone, argillaceous siltstone, and mudstone are deposited along the underwater distributary channel farther out. Drilling coring observation shows that there are many parallel- and cross-beddings in the cores, and the grain size curve shows a common two-stage type (Figure 3). Curves such as natural gamma, resistivity, and sonic time difference show box- or bell-shaped features, indicating that the channel water flow has a strong sorting effect on sand bodies and bringing out and reforming fine-grained materials.

The inter-distributary bay is formed by the deposition of fine-grained silt mudstone and mudstone in a relatively quiet still water environment (Zhang et al., 2006; Wang and Wang., 2021; Xue et al., 2021; Yang et al., 2021). Drilling and coring observation of cores can show the development of horizontal bedding, lenticular bedding, and a few waves forming ripples. At the same time, plant debris and thin coal seams can be seen in the cores. The natural gamma and sonic time difference curves are all zigzag or small peaks with small fluctuations, reflecting the sedimentary characteristics of argillaceous components (Zeng et al., 2007; Yin and Wu., 2020; Zhang et al., 2020).

Sand body distribution characteristics

The sand bodies of the Chang 8 Member in the study area are relatively developed, and the continuity of sand bodies along the strike of the provenance is good (Figure 4). The thickness of the Chang 8_1 sand body is distributed between 5 and 45 m, with an average thickness of 20.5 m. The hydrocarbons are distributed in the upper, middle and lower parts of the Chang 8_1 oil group. The thickness of the Chang 8_2 sand body is distributed between 5 and 40 m, with an average thickness of 23.1 m. A set of relatively thick sand bodies developed in the upper part with good continuity, which is one of the main oil-rich sand layers in this area. Due to the frequent oscillation of the paleochannel, the multi-layered sand bodies develop vertically, and the sand bodies are not well connected in the lateral direction (Figure 4).

Petrological features

The underwater distributary channel of the delta front controls the scale of the reservoir sand bodies in the Chang 8 Member, and the formed sandstones are relatively simple in composition and micro-structures. The reservoirs are dominated by fine sandstone, silty sandstone and siltstone, and are generally characterized by low porosity, low permeability, low oil saturation, and low oil and gas production.

(1) Composition and content of debris components

The main mineral component in the sandstone clastic component is feldspar, accounting for 37–61%, with an average of 51.3%, followed by quartz, accounting for 15–37%, with an average of 23.5%, mainly single crystal quartz. The debris content is 1–16%, with an average of 5.5%. The rock debris are mainly metamorphic debris, the content is generally 1–8%, and

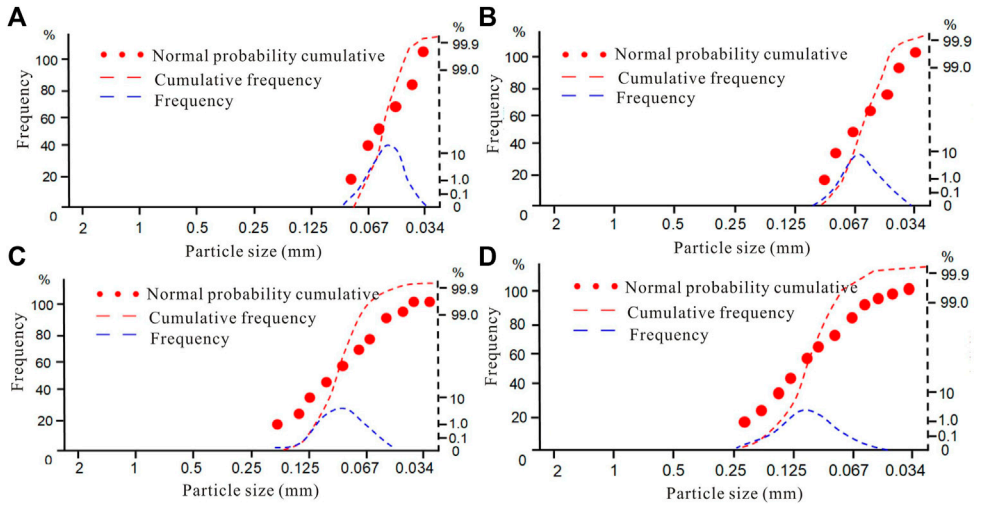

FIGURE 3
Probability accumulation curve of sandstone grain size in the Chang 8 Member of the study area. Notes: **(A)** Well L141, 1,534.2 m; **(B)** Well L143, 1,527.91 m; **(C)** Well L147, 1,449.12 m; **(D)** Well F100, 1,426.52 m.

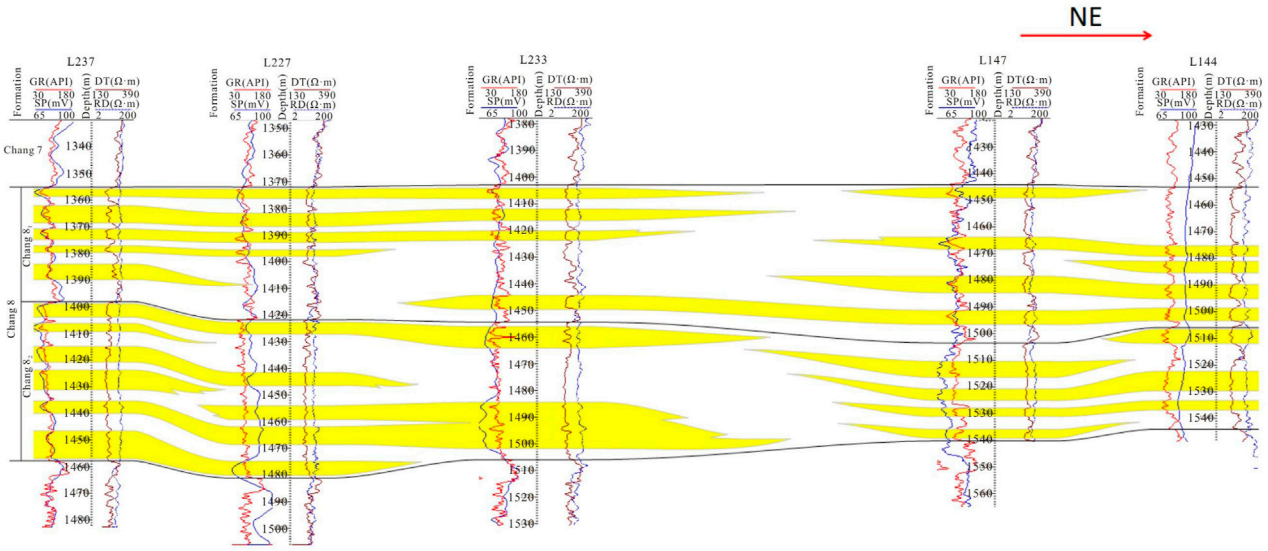

FIGURE 4
Profile of the sand layers (yellow) passing through Wells L237~L144.

the average is 3.4%. Followed by sedimentary rock debris, the content is generally 1–16%, with an average of 1.6%. Magmatic rock debris is the least, and the content is generally 2–5%, with an average of 0.5%; in addition, the content of mica varies greatly, with a content of 1–6%, with an average of 3.6%. The sandstone of the Chang 8 Member in the study area is mainly feldspar sandstone, followed by lithic feldspar sandstone (Figure 5).

(2) Composition and content of interstitials components

The content of cement was distributed between 4.1 and 26%, with an average of 14.91%. The matrix components are mainly mud, and the cements are mainly siderite, calcite, authigenic clay minerals (chlorite, illite, illite/smectite, etc.) and hydromica, followed by secondary growth of quartz and feldspar.

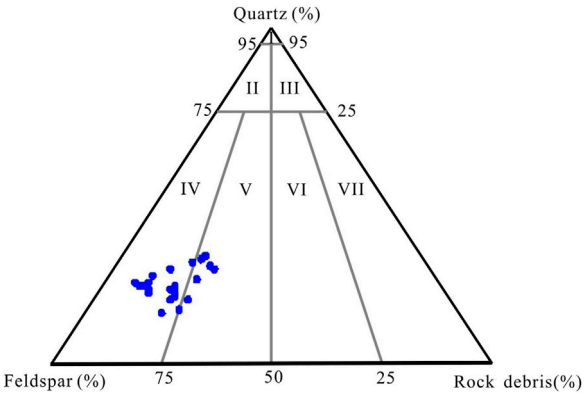

FIGURE 5
Classification triangular map of the Chang 8 sandstone in the study area. Notes: I-quartz sandstone; II-feldspar quartz sandstone; III-lithic quartz sandstone; IV- feldspar sandstone; V-lithic feldspar sandstone; VI- feldspar lithic sandstone; VII-lithic sandstone.

(3) Structural features

According to the identification of a large number of cast thin sections and the results of image particle size analysis, the clastic particles of the Chang 8 reservoir sandstone in the study area are mostly sub-angular-sub-circular, with moderate-to-good sorting, particle support, and line or point-line contacts. The local particles are in concave-convex contact, and the long axes are arranged in a slightly fixed direction.

The main types of cementation are pore-type and membrane-pore type cementation, followed by membrane type and pore-regenerative type cementation, and vitiated cementation can be seen locally. The particle size of most clastic particles is between 0.0625 and 0.25 mm, accounting for 82.14% of the statistical samples, and the median particle size is between 0.05 and 0.15 mm, which is dominated by fine sandstone, followed by silt-fine sandstone.

Discussion

Evaluation of diagenesis

From the perspective of the contribution of diagenesis to reservoir pores, it can be divided into: constructive and destructive diagenesis (Corbett et al., 1987; Chen et al., 1988).

(1) Constructive diagenesis

Constructive diagenesis is the diagenesis that increases the porosity and permeability of the reservoir, which include dissolution, metasomatism, and rupture (Gai et al., 2016; Li et al., 2018; Dong et al., 2020; Liu et al., 2021b).

① Dissolution

The Chang 8 sandstone reservoir in the study area contains a large amount of feldspar, zeolite, calcite and other easily soluble components, which can lead to the dissolution of sandstone components under certain circumstances. Due to the various changes in the environment of the rock, when the fluid in the pore medium has moderate organic acid content and geothermal conditions, some feldspars will be dissolved, resulting in secondary dissolution pores (Figure 6a~b). When the burial depth of the reservoir exceeds 2 km, the strong compaction also aggravates the dissolution. Mechanical dissolution will produce a large amount of H_2SO_4, which can promote the dissolution of quartz and feldspar components.

② metasomatism

Metasomatism is common in the Chang 8 reservoir sandstone in this area, including the alteration of clastic particles and the replacement of clastic particles by cement. The metasomatism of calcite to feldspar can be observed in the target layer, and it can also be seen that the edges of quartz grains are replaced by chlorite. During the metasomatism process, no new substances are produced, and no loss of mineral components occurs, so it has little effect on the quality of the reservoir (Figures 6C, D).

③ rupture

During core observation and thin section identification, various fractures formed by rock instability and fracture can be seen, including structural fractures and interlayer tension fractures (Figure 6E). The production scale of fractures varies, including obvious fractures that can be clearly observed with the naked eye, micro-fractures that can only be described under a microscope, and even hidden fractures or ultra-fine fractures that are difficult to observe under a microscope. The development of fractures can improve the porosity and permeability of the reservoir sandstone to a certain extent, and is also one of the important factors causing the strong heterogeneity of the Chang 8 reservoir in this area.

(2) Destructive diagenesis

Destructive diagenesis can increase the diagenesis of reservoir porosity and permeability, which includes mechanical compaction and cementation (Lima and Deros., 2003; Lommatzsch et al., 2015; Li et al., 2020).

① Mechanical compaction

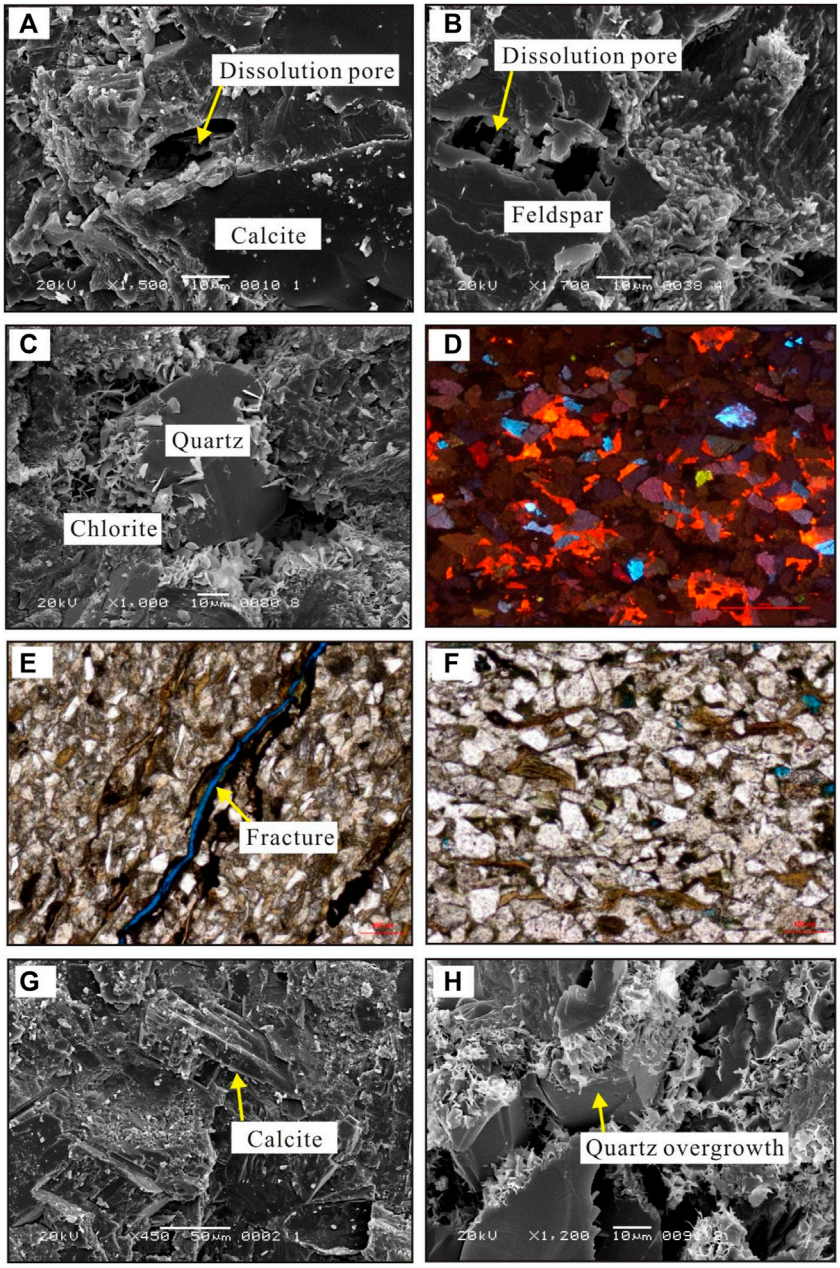

FIGURE 6
Images of microscopic features of different types of pores in the Chang 8 Member. Notes: **(A)** Calcite crystals are dissolved to form dissolution pores (Well L227, 1,429.41 m); **(B)** Feldspar particles were dissolved to form intragranular dissolution pores (Well L237, 1,412.67 m); **(C)** The edge of quartz crystal is replaced by chlorite, (Well L236, 1,412.68 m); **(D)** Feldspar particles were replaced by calcite, (Well L237, 1,412.17 m); **(E)** There are micro-fractures along the bedding direction (Well L227, 1,429.15 m); **(F)** Mica was compacted and deformed, (Well L237, 1,412.59 m); **(G)** Calcite crystals are filled between the detrital grains (Well L227, 1,429.15 m); **(H)** The secondary increase of quartz particles tends to be euhedral (Well L236, 1,415.85 m).

Mechanical compaction runs through the entire process of the burial diagenetic stage, and is one of the main reasons for the reduction of sandstone porosity (McBride., 1989; Moos and Zoback., 1990; Muhammad et al., 2014; Mirzaei-Paiaman and Ghanbarian., 2021). The main manifestations of compaction are: I-plastic deformation, distortion and pseudo-hybridization of I-plastic particles (mica, mudstone, epimetamorphic rock, and volcanic rock debris) (Figure 6F); II-brittle micro-cracks on the surface of rigid particles (quartz, feldspar, etc.) and their displacement and rearrangement; III-compacted directional

fabric, feldspar and mica are often oriented along the long axis direction; Ⅳ-tight packing of debris particles.

② cementation

There are three types of cementation in the Chang 8 clastic rock reservoir in the study area: carbonate, clay mineral and siliceous cementations (Qie et al., 2021; Tong et al., 2012; Zhao et al., 2020; Zeng et al., 2013). Calcite cementation is the most common in the Chang 8 sandstone reservoirs, and is widely distributed in sandstone. The content of carbonate cement in the sandstone of the oil interval is relatively low, generally 0.5–3%. It is usually partially filled with pores or flaky or continuously distributed in flaky shape, which has little effect on porosity loss. The carbonate content in the poor reservoir and tight sandstone is higher, and its content can reach 10–20%. The carbonates with large conjoined crystals fill most or even all of the intergranular pores and replace the clastic particles and interstitials such as feldspar and debris components. Furthermore, the primary intergranular pores are almost completely lost and become a dense barrier (Figure 6G).

The clay minerals include chlorite, illite/smectite, illite, and kaolinite in the clastic reservoirs of the Chang 8 Member in the study area. Among them, the most common one under scanning electron microscope is chlorite, whose content is generally 4–6%, with an average content of 5.55% and a maximum of more than 10%. Among the clay minerals, the average relative content of chlorite can reach 44.3%, followed by illite/smectite mixed layer and illite, with an average content of 2.27 and 2.25%, respectively; the content of kaolinite is the least, with an average content of 1.1%.

The siliceous cement is also widely distributed in the Chang 8 sandstone in this area, and the content is generally 0.5–2%, with an average of 1.0%. Under the scanning electron microscope, secondary enlarged siliceous cementation of quartz can be seen in the clastic rock reservoirs in the study area (Figure 6H), and the secondary enlarged edges of quartz show different colors. Overall, the development of siliceous cementation in the Yanchang Formation sandstone is relatively weak, and the average primary intergranular pores lost by siliceous cementation is 1.0%. However, siliceous cement will cause permanent damage to the pores.

(3) Diagenetic stage

According to previous studies, R_o<0.5% represents early diagenetic stage, R_o = 0.5–1.3% represents middle diagenetic stage A, R_o = 1.3–2.0% represents middle diagenetic stage B. Combined with the diagenetic mineral type and formation sequence of the I/S mixed layer clay in the Chang 8 sandstone in the study area, the vitrinite reflectance (R_o) in the mudstone in the study area is between 0.5 and 1.3%. Therefore, it can be determined that the Chang 8 reservoir in this area has entered the middle diagenetic stage A.

Microscopic pore structures of reservoir

(1) Pore types

The pore types of the target tight sandstone reservoir include intergranular pores, intragranular pores, interstitial pores and fractured pores. According to its origin, it can be divided into three categories: primary pores, secondary pores and fractures.

① Primary pores

Primary pores are the pores formed during the deposition of rocks, including primary intergranular pores and remaining intergranular pores (Price., 1966; Nelson., 1985; Qiao et al., 2020; Radwan and Sen., 2021a; Radwan and Sen., 2021b). Analysis and tests show that the primary pores in the Chang 8 reservoir in the study area mainly develop residual intergranular pores. This type of pore refers to a kind of pore that is not subject to obvious dissolution between skeleton particles due to normal compaction and cementation in the process of diagenetic evolution. Under the microscope, the particles around the pores have no obvious corrosion marks. Its shape is a triangular or irregular polygonal gap (Figures 7A, B).

② Secondary pores

Secondary pores include pores formed by diagenesis such as leaching, dissolution, and metasomatism.

Intergranular dissolution pores are secondary pores formed between particles after the dissolution of rock particles or cements (Shi et al., 2004; Xia et al., 2020; Yoshida and Santosh., 2020; Wang et al., 2021). They are mostly irregular under the microscope, with serrated or harbour-shaped edges. Intragranular dissolution pores are mainly secondary pores generated by local dissolution of feldspar or debris particles, that is, the particles themselves are partially dissolved. Through the observation of cast thin sections and scanning electron microscope, secondary pores generated by local dissolution of feldspar and cement particles are mainly seen in the Chang 8 sandstone in the area (Figures 7C, D). Under the microscope, the dissolution of feldspar particles is more common to form dissolved intergranular pores, and the pores are usually filled with various clay and crystalline minerals, resulting in finer pores in the reservoir and poor pore throat structures.

Intercrystalline pores mainly include intercrystalline micropores formed by the recrystallization of clay minerals,

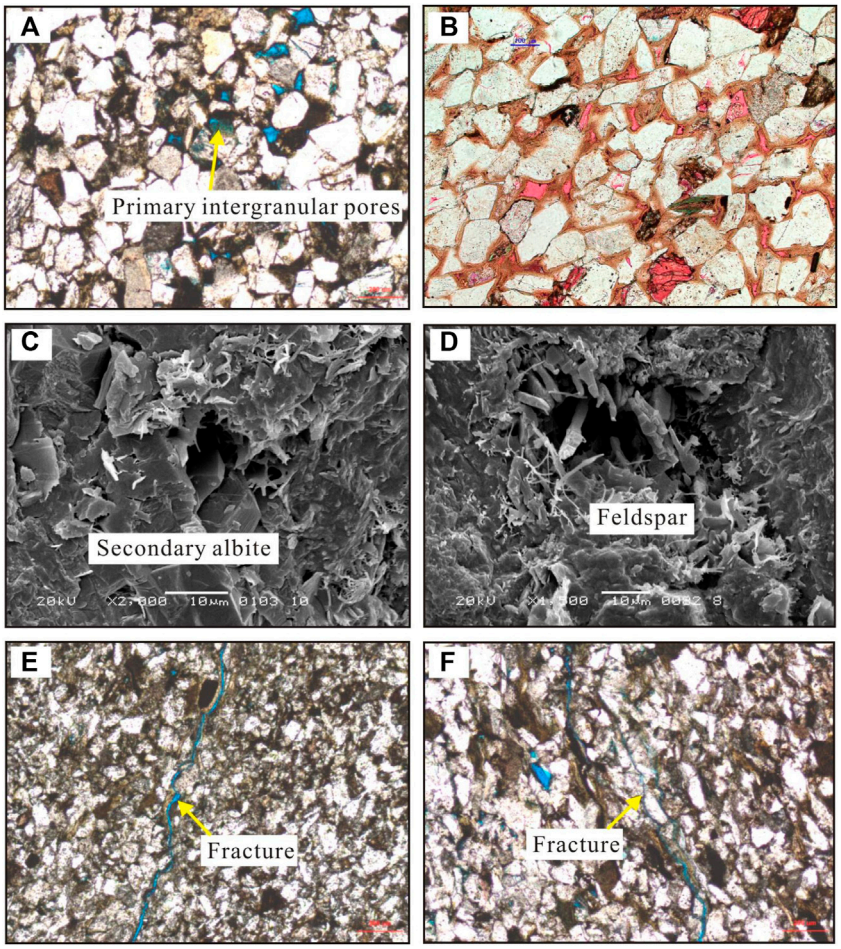

FIGURE 7
Microscopic characteristics of different types of pores in the Chang 8 reservoirs in the study area. Notes: **(A)** Well L227, residual intergranular pores, 1,429.48 m; **(B)** Well L136, residual intergranular pores, 1,527.54 m; **(C)** Well L236, secondary albite crystals in dissolution pores, 1,420.39 m; **(D)** Well L237, hair-like illite is attached to the feldspar dissolution pores, 1,417.91 m; **(E)** Well L237, micro-fractures developed between rock grains, 1,414.25 m; **(F)** Well L236, micro-fractures formed between rock grains, 1,420.46 m.

such as leaf-shaped chlorite intercrystalline micropores, irregular flaky or silky illite intercrystalline micropores, and illite intercrystalline micropores. . Such pores are generally small and poorly connected, and are of little significance for hydrocarbon accumulation.

③ fractures

Fractured pores include rock fissures and grain fissures, which are long and narrow pores and fissures formed by tectonic, mechanical compaction and shrinkage transformation of rocks. Such kind of pores are only developed in local sandstones, and are mainly interlayer horizontal fractures. Fractures develop along layers enriched with biotite or plant debris, and a small number of compression and tensional fractures of oblique bedding can be seen. The opening of microscopic cracks is generally less than 10–20 μm. Statistics show that the opening of the filling crack is relatively large and irregular, and the opening value of the same crack does not change much. The mesh-like micro-cracks are curved, and the opening value is also small. Generally, micro-fractures with an opening greater than 0.1 μm can become effective fractures for oil and gas migration. The opening of micro-fractures in this area is more than 0.1 μm, which can be used as oil and gas storage spaces and oil and gas seepage channels, and become effective fractures (Figures 7E, F).

The development of fractures can improve the porosity and permeability of the reservoir sandstone to a certain extent, and is also one of the important factors causing the strong heterogeneity of the Chang 8 reservoir in this area.

(2) Pore structure features

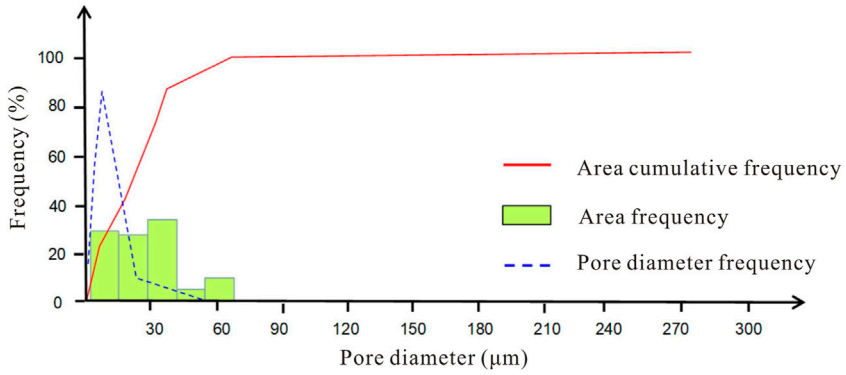

FIGURE 8
Statistical histogram of reservoir pores in the Chang 8 Member in the study area. Well L227, 1,429.15 m.

TABLE 1 Classification standard for pore and throat size of the Chang 8 reservoir in the study area (after Tang et al., 2014).

Pore level	Average pore diameter (μm)	Throat level	Average throat radius (μm)
Macropores	>80	Coarse throats	>3.0
Mesopores	80–50	Medium thin throats	3.0–1.0
Small pores	50–10	Thin throats	1.0–0.5
Thin pores	10–0.5	Micro - thin throats	0.5–0.2
Micropores	<0.5	Micro throats	<0.2

The pore structures of the reservoir rock refer to the geometry, size, distribution and interconnection of the pores and throats of the rock. The properties of the pore structure directly affect the storage performance of the reservoir rock.

Pore analysis of cast images shows that the pores in the Chang 8 reservoir in the study area are poorly developed, and the surface porosity is generally 0.3–2.0%, with an average of 1.33%. Pore shapes are mostly triangular, quadrilateral and irregular. The pore size distribution in a single sample ranges from 5 μm to more than 60 μm, the average pore size is generally 10–30 μm, and the arithmetic mean is 27.45 μm. Therefore, the pores belong to medium to small pores (Figure 8).

Based on the data of rock casting thin section, image pores and scanning electron microscope, the pore structures of the reservoir sandstone of the Chang 8 oil layer group in this area are divided into five types (Table 1).

Influencing factors of physical properties

The Chang 8 Member in the study area developed low-porosity-ultra-low permeability reservoirs. The reasons for their formation are complex and the result of the coupling of various geological factors.

(1) Sedimentation

Sedimentation is the basis for reservoir formation. The regional structure of this area is relatively gentle, and the distribution of oil reservoirs is mainly controlled by the delta front subfacies. The underwater distributary channel sand bodies of the delta front are good oil and gas reservoirs. Usually in the main channel area with good contiguousness and large thickness, the sand body is well sorted and the grain size is coarse. These areas are also blocks with high values of reservoir porosity and permeability, and the oil-bearing properties of the reservoirs are generally good (Figure 9).

(2) Burial compaction

As the overlying sediment thickens, the burial depth increases and the original porosity decreases. Besides being related to the burial depth, there are a lot of mica and epimetamorphic rock debris in the Chang 8 sandstone. During the compaction process, these plastic particles are easily deformed to form pseudo-hetero-bases to fill the original intergranular pores and reduce the physical properties of the reservoir. The analysis shows that there

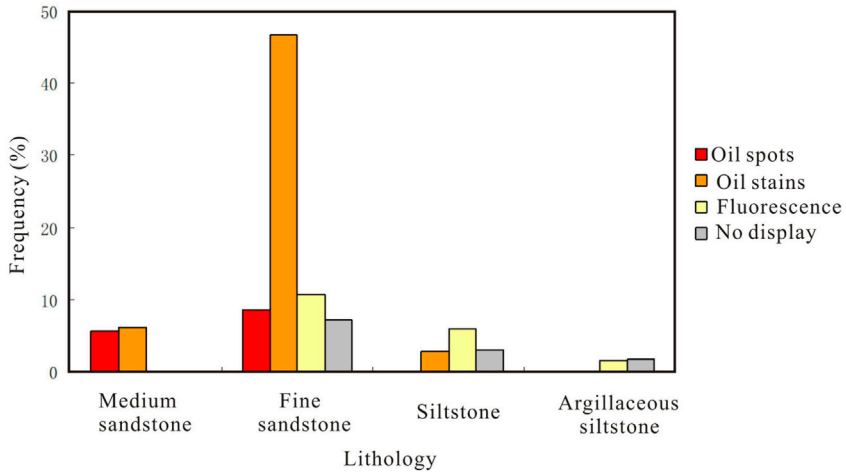

FIGURE 9
Coupling relationship between physical properties and lithology of the Chang 8 Member of Yanchang Formation.

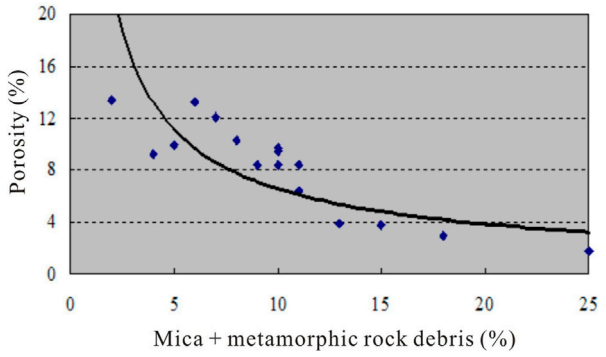

FIGURE 10
Relationship between the content of mica + metamorphic rock debris and porosity in the Chang 8 Member.

is a negative correlation between the content of detrital mica and porosity (Figure 10).

(3) Cementation

Cementation is the main reason affecting the physical properties of the Chang 8 reservoir, and the reduction in porosity can reach about 10% on average. Among all kinds of cementation, the effect of carbonate cementation (calcite, dolomite) is the most obvious. The carbonate cement content in the Chang 8 reservoir in the study area is 1–30%, with an average of 6.5%. The core analysis results show that the carbonate content has a negative relationship with the physical properties of the reservoir, and the higher the carbonate content, the worse the reservoir physical properties (Figure 11).

(4) Dissolution

Dissolution is the main constructive diagenesis. It mainly occurs in the middle-late diagenesis. During the thermal maturation of organic matter, a large amount of organic acid is produced, which dissolves aluminosilicate minerals such as feldspar and debris components. The secondary pores formed by dissolution account for 10–40% of the total surface porosity, with an average of 24%.

Controlling factors for hydrocarbon distribution

The Chang seven and Chang nine source rocks in the study area have wide distribution, large thickness and high hydrocarbon abundance. The sedimentary thickness of the underwater distributary channel sand in the Chang 8 delta front is relatively large, and it is in direct contact with the Chang nine and Chang seven source rocks. Therefore, the Chang 8 Member has the “innate advantageous conditions” for hydrocarbon accumulation.

(1) Controlling effect of local structures on hydrocarbon distribution

The westward dipping tectonic setting of the northern Shaanxi Slope provides the basic conditions for the migration of oil and gas to the eastern updip direction. The regional

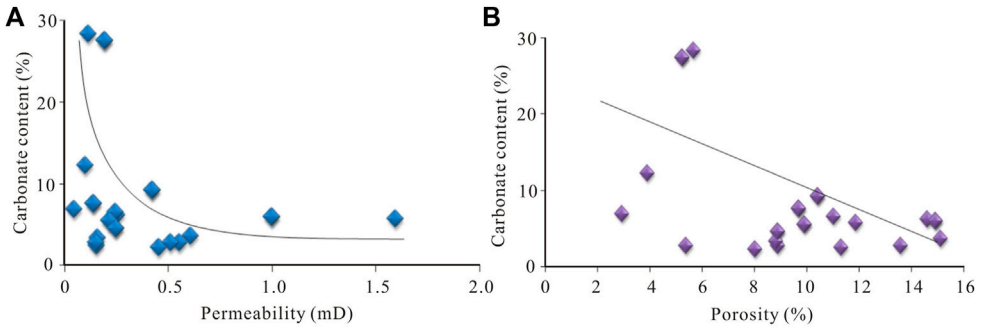

FIGURE 11
Relationship between physical parameters and carbonate content in the target layer. Noets: **(A)** Relationship between permeability and carbonate content; **(B)** Relationship between porosity and carbonate content.

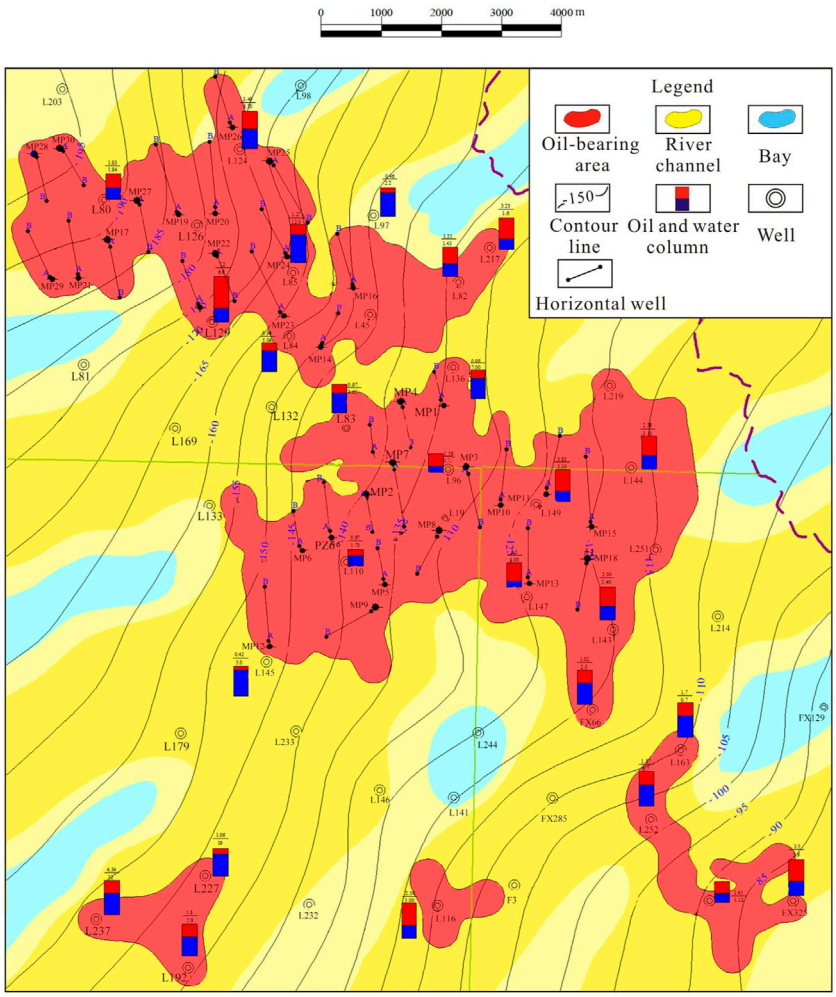

FIGURE 12
Superimposed relationship between the distribution of oil-bearing areas and structures and sedimentary facies (top of the Chang 8_2 sub-member).

structure of this area is a gentle west-dipping monocline, which slopes slightly to the northwest direction and develops a series of nose-shaped uplifts. In addition, the changes of lithology and physical properties in the updip direction of the structure form the blocking conditions for the continued migration of oil and gas, so the oil and gas can form various lithologic reservoirs in the updip direction of the structure. It can be seen from Figure 12 that the central and southern oil reservoirs are mainly distributed in the structural high parts; while some oil reservoirs in the northern part are distributed in relatively low parts. The production capacity of the central and southern reservoirs is significantly higher than the northern one. Therefore, the oil and gas enrichment degree is higher in the high structural parts.

(2) Controlling effect of sedimentary on hydrocarbon distribution

The Chang 8 Member in the study area is a delta front deposit, and mainly develops two microfacies of underwater distributary channel and underwater interdistributary bay. The oil reservoirs are mainly enriched in the main channel area, and the distribution of the oil reservoirs is obviously controlled by the change of the sedimentary facies belt (Figure 12). In addition, the main body of the reservoir is mainly distributed along the distributary channel of the delta front, and most of the distributary channel sandstone is more than 20 m thick. Horizontally, the multi-layer thick sand body distribution area is the main part of oil and gas accumulation. However, the reservoirs formed on the flanks of underwater distributary channels are thin and poorly sorted, which is not conducive to hydrocarbon accumulation.

Conclusion

1) The Chang 8 Member in the study area is a typical delta front subfacies deposit, including distributary channel and inter-distributary bay microfacies. The constructive diagenesis of the Chang 8 Member include dissolution, metasomatism and rupture; while the destructive diagenesis include mechanical compaction and cementation. The Chang 8 reservoir has entered the middle diagenetic stage A.

2) The factors affecting the physical properties of tight oil reservoirs include deposition, compaction, cementation and dissolution. The secondary pores formed by dissolution account for 10–40% of the total surface porosity, with an average value of 24%.

3) Local structures and sediments have significant control over hydrocarbon accumulation. The westward dipping tectonic setting of the northern Shaanxi Slope provides the basic conditions for the migration of oil and gas to the eastern updip direction. The changes of lithology and physical properties in the updip direction of the structure form the blocking conditions for the continued migration of oil and gas, which is conducive to the accumulation of oil and gas.

4) The main oil reservoirs are mainly distributed along the distributary channel of the delta front, and most of the distributary channel sandstone is more than 20 m thick. The distribution area of thick sand body with multiple layers in the lateral direction is the main part of oil and gas accumulation. However, the reservoirs formed on the flanks of underwater distributary channels are thin and poorly sorted, which is not conducive to the accumulation of hydrocarbons.

Data availability statement

The original contributions presented in the study are included in the article/supplementary material further inquiries can be directed to the corresponding author.

Author contributions

BL is responsible for the idea and writing of this paper and BZ, DW, CD, and FW are responsible for the logging interpretation and the experiments.

Conflict of interest

Authors BL and DW were employed by the Development Department, Yanchang Oifield Co., Ltd., author BZ was employed by the Zhidan Oil Production Plant, Yanchang Oilfield Co., LTD., author CD was employed by the Yulin Refinery, Yanchang Petroleum (Group) Co. LTD., and author FW was employed by the Jingbian Oil Production Plant, Yanchang Oilfield Co., LTD.

Publisher's note

References

Anovitz, L. M., Cole, D. R., Rother, G., Allard, L. F., Jackson, A. J., Littrell, K. C., et al. (2013). Diagenetic changes in macro- to nano-scale porosity in the st. Peter sandstone: an (ultra) small angle neutron scattering and backscattered electron imaging analysis. *Geochim. Cosmochim. Acta* 102, 280–305. doi:10.1016/j.gca.2012.07.035

Bieniawski, Z. T. (1967). Mechanism of brittle fracture of rock. *Int. J. Rock Mech. Min. Sci. Geomechanics Abstr.* 4, 407–423. doi:10.1016/0148-9062(67)90031-9

Cai, M. F. (2020). Key theories and technologies for surrounding rock stability and ground control in deep mining. *J. Min. Strata Control. Eng.* 2 (3), 033037. doi:10.13532/j.jmsce.cn10-1638/td.20200506.001

Cao, L., Yao, Y., Cui, C., and Sun, Q. (2020). Characteristics of *in-situ* stress and its controls on coalbed methane development in the southeastern qinshui basin, north china. *Energy Geosci.* 1 (1–2), 69–80. doi:10.1016/j.engeos.2020.05.003

Chalmers, G., Bustin, R. M., and Powers, I. (2009). *A pore by any other name would be as small: The importance of meso-and microporosity in shale gas capacity/*. Denver, Colorado: AAPG Annual Convention and Exhibition, 7–10.

Chalmers, G., and Bustin, R. M. (2007). The organic matter distribution and methane capacity of the lower cretaceous strata of northeastern british columbia, canada. *Int. J. Coal Geol.* 70 (1-3), 223–239. doi:10.1016/j.coal.2006.05.001

Chen, G. B., Li, T., Yang, L., Zhang, G. H., Li, J. W., and Dong, H. J. (2021). Mechanical properties and failure mechanism of combined bodies with different coal-rock ratios and combinations. *J. Min. Strata Control Eng.* 3 (2), 023522. doi:10.13532/j.jmsce.cn10-1638/td.20210108.001

Chen, Q., Zhang, J., Tang, X., Li, W., and Li, Z. (2016). Relationship between pore type and pore size of marine shale: an example from the sinian - cambrian formation, upper yangtze region, south china. *Int. J. Coal Geol.* 158, 13–28. doi:10.1016/j.coal.2016.03.001

Chen, Z. M., Zhang, S. L., and Wan, L. G. (1988). Gulong qingshankou mudstone north of structural cracks and reservoir distribution and prediction. *Pet. Technol.* 9, 5

Corbett, K. P., Friedman, M., and Spang, J. (1987). Fracture development and mechanical stratigraphy of Austin Chalk, Texas. *Am. Assoc. Pet. Geol.* 71, 17

Curtis, M. E., Cardott, B. J., Sondergeld, C. H., and Rai, C. (2012). Development of organic porosity in the woodford Shale with increasing thermal maturity. *Int. J. Coal Geol.* 103, 26–31. doi:10.1016/j.coal.2012.08.004

Dong, S., Zeng, L., Lyu, W., Xia, D., Liu, G., Wu, Y., et al. (2020). Fracture identification and evaluation using conventional logs in tight sandstones: a case study in the Ordos Basin, china. *Energy Geosci.* 1 (3–4), 115–123. doi:10.1016/j.engeos.2020.06.003

Gai, S., Liu, H., He, S., Mo, S., Chen, S., Liu, R., et al. (2016). Shale reservoir characteristics and exploration potential in the target: a case study in the longmaxi formation from the southern sichuan basin of China. *J. Nat. Gas Sci. Eng.* 31, 86–97. doi:10.1016/j.jngse.2016.02.060

Hong, D., Cao, J., Wu, T., Dang, S., Hu, W., Yao, S., et al. (2020). Authigenic clay minerals and calcite dissolution influence reservoir quality in tight sandstones: insights from the central junggar basin, NW China. *Energy Geosci.* 1 (1–2), 8–19. doi:10.1016/j.engeos.2020.03.001

Houben, M. E., Desbois, G., and Urai, J. L. (2013). Pore morphology and distribution in the shaly facies of opalinus clay(mont terri, Switzerland): insights from representative 2D BIB-sem investigations on mm to nm scale. *Appl. Clay Sci.* 71, 82–97. doi:10.1016/j.clay.2012.11.006

Lai, J., and Wang, G. (2015). Fractal analysis of tight gas sandstones using high-pressure mercury intrusion techniques. *J. Nat. Gas Sci. Eng.* 24, 185–196. doi:10.1016/j.jngse.2015.03.027

Lai, J., Wang, G. W., Wang, Z. Y., Chen, J., Pang, X. J., Wang, S. C., et al. (2018). A review on pore structure characterization in tight sandstones. *Earth-Science Rev.* 177, 436–457. doi:10.1016/j.earscirev.2017.12.003

Lan, S. R., Song, D. Z., Li, Z. L., and Liu, Y. (2021). Experimental study on acoustic emission characteristics of fault slip process based on damage factor. *J. Min. Strata Control Eng.* 3 (3), 033024. doi:10.13532/j.jmsce.cn10-1638/td.20210510.002

Li, D. Y., Wong, L. N. Y., Liu, G., and Zhang, X. P. (2012). Influence of water content and anisotropy on the strength and deformability of low porosity meta-sedimentary rocks under triaxial compression. *Eng. Geol.* 126, 46––66. doi:10.1016/j.enggeo.2011.12.009

Li, H. (2022). Research progress on evaluation methods and factors influencing shale brittleness: a review. *Energy Rep.* 8, 4344–4358. doi:10.1016/j.egyr.2022.03.120

Li, L., Huang, B., Li, Y., Hu, R., and Li, X. (2018). Multi-scale modeling of shale laminas and fracture networks in the Yanchang Formation, southern Ordos Basin, China. *Eng. Geol.* 243, 231–240. doi:10.1016/j.enggeo.2018.07.010

Li, X., He, Y., Huo, M., Yang, Z., Wang, H., Song, R., et al. (2019). Simulation of coupled thermal-hydro-mechanical processes in fracture propagation of carbon dioxide fracturing in oil shale reservoirs. *Energy Sources Part A Recovery Util. Environ. Eff.* 23, 1–20. doi:10.1080/15567036.2019.1676329

Li, Y., Zhou, D., Wang, W., Jiang, T., and Xue, Z. (2020). Development of unconventional gas and technologies adopted in China. *Energy Geosci.* 1 (1–2), 55–68. doi:10.1016/j.engeos.2020.04.004

Lima, R. D., and Deros, L. F. (2003). The role of depositional setting and diagenesis on the reservoir quality of devonian sandstones from the solimões basin, brazilian amazonia. *Mar. Petroleum Geol.* 19, 1047. doi:10.1016/s0264-8172(03)00002-3

Liu, B., He, S., Meng, L., Fu, X., Gong, L., Wang, H., et al. (2021a). Sealing mechanisms in volcanic faulted reservoirs in xujiaweizi extension, northern songliao basin, northeastern china. *Am. Assoc. Pet. Geol. Bull.* 105, 1721–1743. doi:10.1306/03122119048

Liu, B., Sun, J., Zhang, Y., He, J., Fu, X., Yang, L., et al. (2021b). Reservoir space and enrichment model of shale oil in the first member of Cretaceous qingshankou formation in the changling sag, southern Songliao Basin, NE China. *Petroleum Explor. Dev.* 48 (3), 608–624. doi:10.1016/S1876-3804(21)60049-6

Liu, Y., Chen, L., Tang, Y., Zhang, X., and Qiu, Z. (2022). Synthesis and characterization of nano-SiO_2@octadecylbisimidazoline quaternary ammonium salt used as acidizing corrosion inhibitor. *Rev. Adv. Mater. Sci.* 61 (1), 186–194. doi:10.1515/rams-2022-0006

Liu, Z. L., Fan, A. P., Li, Y. J., Du, Z. W., Zhao, Z. J., and Zhang, T. (2015). Constraints of clastic component difference on diagenesis: a case study of sandstone reservoirs in dong-2 block of the sulige gasfield, Ordos Basin. *Nat. Gas. Ind.* 35, 30–38.

Liu, B, B., Yang, Y., Li, J., Chi, Y., Li, J., Fu, X., et al. (2020). Stress sensitivity of tight reservoirs and its effect on oil saturation: a case study of lower cretaceous tight clastic reservoirs in the hailar basin, northeast China. *J. Petroleum Sci. Eng.* 184, 106484. doi:10.1016/j.petrol.2019.106484

Liu, J, J., Yang, H., Bai, J., Wu, K., Zhang, G., Liu, Y., et al. (2020). Numerical simulation to determine the fracture aperture in a typical basin of China. *Fuel* 283, 118952. doi:10.1016/j.fuel.2020.118952

Lommatzsch, M., Exner, U., Gier, S., and Grasemann, B. (2015). Dilatant shear band formation and diagenesis in calcareous, arkosic sandstones, Vienna Basin (Austria). *Mar. Petroleum Geol.* 62, 144–160. doi:10.1016/j.marpetgeo.2015.02.002

Lorenz, J. C., and Finley, S. J. (1991). Regional fractures: fracturing of mesaverde reservoirs in the piceance basin, Colorado. *Am. Assoc. Pet. Geol. Bull.* 75, 1738–1757.

Mahmoodi, S., Abbasi, M., and Sharifi, M. (2019). New fluid flow model for hydraulic fractured wells with non-uniform fracture geometry and permeability. *J. Nat. Gas Sci. Eng.* 68, 102914. doi:10.1016/j.jngse.2019.102914

Mahmud, H., Hisham, M., Mahmud, M., Leong, V., and Shafiq, M. (2020). Petrophysical interpretations of subsurface stratigraphic correlations, baram delta, sarawak, malaysia. *Energy Geosci.* 1 (3–4), 100–114. doi:10.1016/j.engeos.2020.04.005

McBride, E. F. (1989). Quartz cement in sandstones: a review. *Earth. Sci. Rev.* 26, 69–112. doi:10.1016/0012-8252(89)90019-6

Mirzaei-Paiaman, A., and Ghanbarian, B. (2021). A new methodology for grouping and averaging capillary pressure curves for reservoir models. *Energy Geosci.* 2 (1), 52–62. doi:10.1016/j.engeos.2020.09.001

Moos, D., and Zoback, M. D. (1990). Utilization of observations of well bore failure to constrain the orientation and magnitude of crustal stresses: application to continental, deep sea drilling project, and ocean drilling program boreholes. *J. Geophys. Res.* 95, 9305. doi:10.1029/jb095ib06p09305

Muhammad, A., Hammerschmidt, U., and Köhler, J. (2014). Thermophysical properties of a fluid- saturated sandstone. *Int. J. Therm. Sci.* 76, 43–50. doi:10.1016/j.ijthermalsci.2013.08.017

Nelson, R. A. (1985). *Geologic analysis of naturally fractured reservoirs: contributions in petroleum geology and engineering*. Houston: Gulf Publishing Company, 320–321.

Nie, H., Li, D., Liu, G., Lu, Z., Hu, W., Wang, Ru., et al. (2020). An overview of the geology and production of the Fuling shale gas field, Sichuan Basin, China. *Energy Geosci.* 1 (3–4), 147–164. doi:10.1016/j.engeos.2020.06.005

Price, N. J. (1966). *Fault and joint development in brittle and semi-brittle rock*. Oxford, England: Pergamon Press, 221–240.

Qiao, J., Zeng, J., Jiang, S., and Wang, Y. (2020). Impacts of sedimentology and diagenesis on pore structure and reservoir quality in tight oil sandstone reservoirs: implications for macroscopic and microscopic heterogeneities. *Mar. Petroleum Geol.* 111, 279–300. doi:10.1016/j.marpetgeo.2019.08.008

Qie, L., Shi, Y. N., and Liu, J. S. (2021). Experimental study on grouting diffusion of gangue solid filling bulk materials. *J. Min. Strata Control Eng.* 3 (2), 023011. doi:10.13532/j.jmsce.cn10-1638/td.20201111.001

Radwan, A. E., Abdelghany, W. K., and Elkhawaga, M. A. (2021). Present-day *in-situ* stresses in southern gulf of suez, egypt: insights for stress rotation in an extensional rift basin. *J. Struct. Geol.* 147. doi:10.1016/j.jsg.2021.104334

Radwan, A. E. (2022). "Chapter Two - three-dimensional gas property geological modeling and simulation," in *Sustainable geoscience for natural gas sub-surface systems*. Editors D. A. Wood and J. Cai (Elsevier), 29–45. Chapter 2 in. doi:10.1016/B978-0-323-85465-8.00011-X

Radwan, A. E., and Sen, S. (2021b). Characterization of *in-situ* stresses and its implications for production and reservoir stability in the depleted El Morgan hydrocarbon field, gulf of suez rift basin, egypt. *J. Struct. Geol.* 148. doi:10.1016/j.jsg.2021.104355

Radwan, A., and Sen, S. (2021a). Stress path analysis for characterization of *in situ* stress state and effect of reservoir depletion on present-day stress magnitudes: reservoir geomechanical modeling in the gulf of suez rift basin, Egypt. *Nat. Resour. Res.* 30, 463–478. doi:10.1007/s11053-020-09731-2

Santosh, M., and Feng, Z. Q. (2020). New horizons in energy geoscience. *Energy Geosci.* 1 (1–2), 1. doi:10.1016/j.engeos.2020.05.005

Shanley, K. W., and Cluff, R. M. (2015). The evolution of pore-scale fluid-saturation in low permeability sandstone reservoirs. *Am. Assoc. Pet. Geol. Bull.* 99, 1957–1990. doi:10.1306/03041411168

Shi, D. S., Li, M. W., Pang, X. Q., Chen, D. X., Zhang, S. W., Wang, Y. S., et al. (2004). Fault-fracture mesh petroleum plays in the zhanhua depressio, bohai bay basin: Part2. Oil-source correlation and secondary migration mechanisms. *Org. Geochem.* 36, 203–223.

Shuai, Y., Zhang, S., Mi, J., Gong, S., Yuan, X., Yang, Z., et al. (2013). Charging time of tight gas in the upper paleozoic of the Ordos Basin, central china. *Org. Geochem.* 64, 38–46. doi:10.1016/j.orggeochem.2013.09.001

Tang, Y., Song, Z., and Zhao, K. (2014). Characteristics and influencing factors of Chang 8 reservoir of Yanchang Formation in western Ordos Basin. *J. Lanzhou Univ. Sci.* 50 (6), 779–785+794. doi:10.13885/j.issn.0455-2059.2014.06.003

Tong, K. J., Zhao, C. M., Lu, Z. B., Zhang, Y. C., Zheng, H., Xu, S. N., et al. (2012). Reservoir evaluation and fracture chracterization of the metamorphicburied hill reservoir in bohai bay basin. *Petroleum Explor. Dev.* 39, 62–69. doi:10.1016/s1876-3804(12)60015-9

Wang, D. L., Hao, B. Y., and Liang, X. M. (2021). Slurry diffusion of singlefracture based on fluid-solid coupling. *J. Min. Strata Control. Eng.* 3 (1), 013038. doi:10.101638/td.20200429.001

Wang, J., and Wang, X. L. (2021). Seepage characteristic and fracture development of protected seam caused by mining protecting strata. *J. Min. Strata Control Eng.* 3 (3), 033511. doi:10.13532/j.jmsce.cn10-1638/td.20201215.001

Xia, Y. X., Lu, C., Yang, G. Y., Su, S. J., Pang, L. N., Ding, G. L., et al. (2020). Experimental study on axial fracture cutting and fracturing of abrasive jet in hard roof hole. *J. Min. Strata Control Eng.* 2, 033522.

Xiao, Z., Ding, W., Liu, J., Tian, M., Yin, S., Zhou, X., et al. (2019). A fracture identification method for low-permeability sandstone based on R/S analysis and the finite difference method: a case study from the Chang 6 reservoir in huaqing oilfield, Ordos Basin. *J. Petroleum Sci. Eng.* 174, 1169–1178. doi:10.1016/j.petrol.2018.12.017

Xu, Y., Zhang, H., and Guan, Z. (2021). Dynamic characteristics of downhole bit load and analysis of conversion efficiency of drill string vibration energy. *Energies* 14, 229. doi:10.3390/en14010229

Xue, F., Liu, X. X., and Wang, T. Z. (2021). Research on anchoring effect of jointed rock mass based on 3D printing and digital speckle technology. *J. Min. Strata Control Eng.* 3 (2), 023013. doi:10.13532/j.jmsce.cn10-1638/td.20201020.001

Yan, D. (2020). *Identification and evaluation of source rock and reservoir in tight oil from the 7th member of Yanchang Formation in the center of Lake basin, Ordos Bain*. Northwest University, 45–48. doi:10.27405/d.cnki.gxbdu.2020.002273

Yang, J. X., Luo, M. K., Zhang, X. W., Huang, N., and Hou, S. J. (2021). Mechanical properties and fatigue damage evolution of granite under cyclic loading and unloading conditions. *J. Min. Strata Control Eng.* 3 (3), 033016. doi:10.13532/j.jmsce.cn10-1638/td.20210510.001

Yin, S., Lv, D. W., and Ding, W. L. (2018). New method for assessing microfracture stress sensitivity in tight sandstone reservoirs based on acoustic experiments. *Int. J. Geomech.* 18 (4), 1–16. doi:10.1061/(asce)gm.1943-5622.0001100

Yin, S., and Wu, Z. (2020). Geomechanical simulation of low-order fracture of tight sandstone. *Mar. Petroleum Geol.* 100, 104359. doi:10.1016/j.marpetgeo.2020.104359

Yoshida, M., and Santosh, M. (2020). Energetics of the solid Earth: an integrated perspective. *Energy Geosci.* 1 (1–2), 28–35. doi:10.1016/j.engeos.2020.04.001

Zeng, L. B., Qi, J. F., and Li, Y. G. (2007). The relationship between fractures and tectonic stress field in the extra low-permeability sandstone reservoir at the south of western sichuan depression. *J. China Univ. Geosciences* 18, 223–231. doi:10.1016/s1002-0705(08)60003-5

Zeng, W. T., Zhang, J. C., Ding, W. L., Zhao, S., Zhang, Y. Q., Liu, Z. J., et al. (2013). Fracture development in paleozoic shale of chongqing area (South China). part one: fracture characteristics and comparative analysis of main controlling factors. *J. Asian Earth Sci.* 75, 251–266. doi:10.1016/j.jseaes.2013.07.014

Zhang, B., Shen, B., and Zhang, J. (2020). Experimental study of edge-opened cracks propagation in rock-like materials. *J. Min. Strata Control Eng.* 2 (3), 033035. doi:10.13532/j.jmsce.cn10-1638/td.20200313.001

Zhang, T., Switzer, P., and Journel, A. (2006). Filter-based classification of training image patterns for spatial simulation. *Math. Geol.* 38 (1), 63–80. doi:10.1007/s11004-005-9004-x

Zhao, Z., Wu, K., Fan, Y., Guo, J., Zeng, B., Yue, W., et al. (2020). An optimization model for conductivity of hydraulic fracture networks in the longmaxi shale, sichuan basin, southwest china. *Energy Geosci.* 1 (1–2), 47–54. doi:10.1016/j.engeos.2020.05.001